Cellulose
https://doi.org/10.1007/s10570-022-04963-2

ORIGINAL RESEARCH

Oil structuring properties of electrospun Kraft lignin/cellulose acetate nanofibers for lubricating applications: influence of lignin source and lignin/cellulose acetate ratio

J. F. Rubio-Valle · C. Valencia · M. Sánchez · J. E. Martín-Alfonso · J. M. Franco

Received: 25 July 2022 / Accepted: 21 November 2022

Abstract In the present work, electrospun Kraft lignin/cellulose acetate nanostructures were produced, assessed and proposed as structuring or thickening agents of castor oil for lubricating applications. Solutions of Kraft lignins (KL) derived from different sources (eucalyptus, poplar and olive tree pruning) and cellulose acetate (CA) were prepared and used as feed for electrospinning. The rheological properties (shear and extensional viscosity), electrical conductivity and surface tension of KL/CA solutions influence the morphology of the electrospun nanofibers, which in turn is affected by the chemical structure and composition of the Kraft lignins. Electrospun KL/CA nanostructures consisting of filament-interconnected nanoparticles, beaded nanofibers or uniform nanofiber mats were able to form gel-like homogeneous fine dispersions by simply mechanically dispersing them into castor oil. The swelling of KL/CA nanofibers in the percolation network was demonstrated. The rheological, tribological and microstructural properties of these oleogels are essentially governed by the morphological characteristics of the electrospun nanostructures, i.e. fiber diameter, number of beads and porosity. Rheological properties of the resulting oleogels may be tailored by modifying the lignin source and KL:CA weight ratio. According to their rheological and tribological properties, KL/CA electrospun nanostructures-based oleogels can be proposed as a sustainable alternative to conventional lubricating greases.

Keywords Bio-lubricating greases · Lignin · Cellulose acetate · Electrospinning · Oleogels · Rheology · Tribology

Introduction

In the last decades, different strategic lines based on the bioeconomy concept have been proposed in order to use renewable resources as industrial raw materials, particularly in the manufacture of different value-added products (Staffas et al. 2013). According to these trends, the bioeconomy and biorefinery concepts have emerged as solutions in response to current environmental and social challenges, reducing the effects of climate change and decreasing the use of fossil fuels (Octave and Thomas 2009; Lewandowski 2018; Lainez et al. 2018). More specifically, in the field of lubricant technology, the new environmental policies and guidelines have prompted strategic changes in the sector (Boyde 2002). Several studies

Supplementary Information The online version contains supplementary material available at https://doi.org/10.1007/s10570-022-04963-2.

J. F. Rubio-Valle · C. Valencia · M. Sánchez · J. E. Martín-Alfonso · J. M. Franco (✉)
Pro2TecS – Chemical Product and Process Technology Research Center, Department of Chemical Engineering and Materials Science, ETSI, Universidad de Huelva, Campus de "El Carmen", 21071 Huelva, Spain
e-mail: franco@uhu.es

Published online: 02 December 2022

have shown that traditional lubricants exert negative effects on the environment and, therefore, new environmentally friendly products that can reduce this impact are demanded (Syahir et al. 2017). In the particular case of lubricating greases, where a thickening agent is required to impart gel-like properties in order to prevent dripping and spattering of lubricant and therefore decrease the frequency of lubrication, the replacement of mineral and synthetic oils with vegetable-derived oils is not enough, but natural and/or biodegradable as well as technologically efficient thickeners and additives are also required. The oil structuring ability of biopolymers such as cellulose and chitosan derivatives or lignocellulosic components is very limited due to their polar chemical nature. Only very few biopolymers, such as ethylcellulose, are able to gel oils directly by the formation of supramolecular structures (Davidovich-Pinhas et al. 2015), but still having serious drawbacks as thickeners in lubricant formulations (Martín-Alfonso et al. 2011). Other strategies involving chemical modifications of biopolymers with diisocyanates or epoxides have been also proposed to induce oil structuration via chemical crosslinking (Gallego et al. 2013; Borrero-López et al. 2018a, 2020; Cortés-Triviño et al. 2019, 2021). Moreover, some distinguishing properties of natural substances that might be employed as special additives in lubricants have been extensively investigated. Among them, the antioxidant capacity of lignin in vegetable oils is worth mentioning here (Jedrzejczyk et al. 2021).

In general, the utilization of lignocellulosic biomass has increased in recent years, being one of the most important among the wide range of natural polymers available (Gnansounou 2010; Sørensen et al. 2013). Unlike other biomasses, such as sugar or starch, lignocellulosic biomass is abundant, low-cost, renewable source, highly distributed, and not dedicated to food consumption (Kobayashi and Fukuoka 2013; Shahzadi et al. 2014; Cai et al. 2017). In addition, several forest species are very suitable for lignocellulosic biomass production, such as Salicaceae (poplars and willows), Myrtaceae (eucalyptus) and Oleaceae (olive trees). One of the most available, renewable and low-cost lignocellulosic wastes produced in Mediterranean countries comes from the pruning of the above-mentioned species (Limayem and Ricke 2012; Romero-García et al. 2014; Ullah et al. 2015). In particular, olive tree prunings are usually removed to maintain the fields clean and avoid the spread of plant diseases by burning or shredding, which produces economic costs and environmental impacts. These factors, combined with their suitable chemical composition, have led to these agricultural residues being proposed as potential raw materials for a broad spectrum of high value-added products (Cara et al. 2008; Negro et al. 2017).

The interest in lignocellulosic biomass is traditionally focused on its high content of cellulose and hemicellulose, which have diverse applications (Borrero-López et al. 2022). However, the use and valorization of lignin have been much less explored (Bajpai 2016), despite it is one of the renewable resources with high potential for industrial use, including the manufacture of high value-added products (Gellerstedt and Henriksson 2008; Laurichesse and Avérous 2014; Pelaez-Samaniego et al. 2016; Xi et al. 2018). This is attributed to the fact that the chemical structure of lignin has not been determined as precisely as that of other biopolymers like, for instance, cellulose, due to difficulties arising in its separation, structural characterization, and compositional analysis (Obst 1983).

Therefore, the utilization of lignin as a potential thickening or structuring agent in a vegetable oil medium is justified as a new way of revalorization (Borrero-López et al. 2018b). Aiming to avoid complex chemical modifications such as those previously mentioned, efficient interaction between lignin and oil can be achieved physically at the nanoscale. Thus, lignin nanostructures, with high porosity, nanometric size, and high surface/volume ratio may have the ability to entrap the oil in the generated voids, thus enhancing the physical interactions. As recently demonstrated (Borrego et al. 2021; Rubio-Valle et al. 2021b), such kinds of lignin nanostructures can be easily generated by electrospinning. However, a high surface-to-volume ratio, i.e. nanofibers, cannot be achieved by feeding only lignin solutions because lignin cannot generate sufficient chain entanglements within the solution as a consequence of its chemical structure and relatively low molecular weight (Diez-Rodríguez et al. 2013). To improve lignin electrospinnability, the multiple approaches found in the literature involve blending with a second polymer (Jia et al. 2018; Svinterikos et al. 2020; Borrego et al. 2021). In this regard, cellulose acetate is herein considered a suitable dopant polymer, as it is able to form nanofibers with relative ease as well as possesses other

interesting properties such as biodegradability, biocompatibility, renewability, etc. (Liu and Hsieh 2002; Teixeira et al. 2020). Accordingly, based on the previous considerations, in the present work, three different Kraft lignins (KL) from eucalyptus, poplar and olive tree pruning, respectively, have been used and evaluated aiming to obtain electrospun lignin/cellulose acetate nanofibers with oil structuring properties. The resulting oleogels have been rheologically and tribologically characterized, and their properties were assessed to propose them as lubricants.

Material and methods

Materials

Kraft lignins from eucalyptus (EKL), poplar (PKL) and olive tree prunings (OKL) were employed as raw materials together with cellulose acetate (CA) to produce electrospun nanostructures. EKL, PKL and OKL were kindly provided by INIA-CSIC (Spain). Detailed information on Kraft lignin isolation, composition, and chemical structure can be found elsewhere (García-Fuentevilla et al. 2022). The most relevant compositional and structural characteristics of these lignin samples are summarized in Table 1. CA (39.8 wt% acetylated, M_n: 30,000 g/mol) was supplied by Merck Sigma-Aldrich S.A. (Germany). *N, N*-Dimethylformamide (DMF) and acetone (Ac) also provided by Merck Sigma-Aldrich S.A. (Germany), were used as solvents in the preparation of KL/CA solutions. Castor oil from Guinama (Valencia, Spain) was used as a base oil to formulate the oleogels. The fatty acid composition and main physical properties of this vegetable oil are described elsewhere (Quinchia et al. 2010).

Table 1 Total lignin content, abundance of lignin β-O-4' substructures expressed per 100 aromatic units (as relative percentage of the total linkages considered), syringyl/guaiacyl (S/G) ratio, weight-average (M_w) and number-average (M_n) molecular weights and polydispersity (M_w/M_n) of the Kraft lignin samples studied (data from (García-Fuentevilla et al. 2022))

	EKL	PKL	OKL
Total lignin content (%)	98.2	91	72
β-O-4' substructures (%)	5.9	1.8	0.3
S/G ratio	7.9	4.7	2.5
M_w (Da)	5285	5445	4780
M_n (Da)	4230	4550	4390
M_w/M_n	1.24	1.19	1.08
Total phenol content (mg GAE/g lignin)	627.43	585.72	295.42

Production of electrospun KL/CA nanostructures

KL/CA solutions were prepared at 30 wt.% of total biopolymer concentration in two different KL:CA weight ratios (9:1 and 7:3). KL and CA were separately dissolved in DMF/Ac mixtures (1:2 v/v), under magnetic stirring (500 rpm) for 24 h, at room temperature (22 ± 1 °C) and, afterwards, both solutions were blended to achieve the final composition.

KL/CA solutions were then electrospun in a DOXA Microfluidics (Spain) chamber. The spinning solution (10 mL) was continuously fed through a plastic syringe with a 21-G needle. The syringe was arranged in a horizontal configuration and connected to a high voltage power source that provided 17 kV. Electrospun nanostructures were collected in an aluminum plate placed at 15 cm from the needle tip. All experiments were conducted at room temperature and constant relative humidity (45 ± 1%).

Preparation of oleogels

Electrospun KL/CA nanostructures were carefully removed from the collector with the help of tweezers and a spatula and directly dispersed in castor oil, at a 15 wt. % concentration, under agitation at room temperature for 24 h. This concentration was selected according to preliminary tests, in order to achieve rheological properties and consistencies similar to those found in conventional lubricating greases. The resulting dispersions were stored at room temperature for further characterization.

Characterization techniques

Characterization of KL/CA solutions

The dynamic viscosity of the EKL/CA solutions was determined under shear, at 25 °C, in an ARES (Rheometric Scientific, UK) controlled-strain rheometer, using a Couette geometry, in a shear rate range of 1–300 s^{-1}.

The extensional viscosity of KL/CA solutions was measured using a CaBER (Thermo-Haake GmbH, Germany) extensional rheometer, at 25 °C. A small drop of the solution was deposited between two parallel plates (4 mm in diameter), which were then suddenly separated vertically, thus creating an unstable filament that flows under the gravity action. The evolution of the filament diameter with time was measured using a laser blade micrometer.

Surface tension measurements were performed in a Sigma 703D (Biolin Scientific, China) force tensiometer, at 25 °C, using a platinum Wilhelmy plate (width 39.24 mm, thickness 0.1 mm). The electrical conductivity of KL/CA solutions was measured using a CE GLP31 conductivity meter (Crison, Spain), at 25 °C.

Characterization of electrospun KL/CA nanostructures

The electrospun nanostructures were analyzed in a JXA-8200 SuperProbe (JEOL, Japan) scanning electron microscope with a secondary electron detector at an acceleration voltage of 15 kV and different magnifications (×4000 and ×10,000). The membranes were previously coated with gold using a sputter coater BTT150 (HHV, UK). FIJI ImageJ analysis software was used to analyze the SEM images. For each sample, 100 random observations were carried out at the same magnification to determine the mean diameter of particles and fibers. In addition, porosity was obtained using the same software by changing the contrast of the micrographs.

Characterization of oleogels

Rheological properties of oleogels were determined in a Rheoscope (TermoHaake, Germany) controlled-stress rheometer, using a serrated plate-plate geometry (20 mm diameter and 1 mm gap). Small-amplitude oscillatory shear (SAOS) tests were performed, inside the linear viscoelastic region, in the frequency range of 0.03–100 rad s^{-1}, at 25 °C. Stress sweeps were previously carried out to determine the extension of the linear viscoelastic regime. Viscous flow tests were performed in a shear rate range of 10^{-2}–10^{2} s^{-1}.

Tribological measurements were carried out in a Physica MCR-501 rheometer (Anton Paar, Austria) fitted with a tribological cell, comprised of a 6.35 mm diameter steel ball that rotates on three 45° inclined rectangular steel plates, where the oleogel samples acting as lubricants were placed. A constant axial load and a rotational speed of 20 N and 10 rpm, respectively, were applied for 10 min. Perpendicular normal force and friction coefficient were determined from the applied axial force and the torsional force measured by the rheometer, according to the geometrical characteristics of the tribological cell (Heyer and Läuger 2009).

The microstructure of the oleogels was analyzed using an AURIGA (Zeiss, USA) scanning electron microscope, with a secondary electron detector at an acceleration voltage of 20 kV. A double fixation protocol with 2.5% glutaraldehyde in 0.1 M cacodylate buffer for 2 h, and 1% osmium tetroxide for 1 h was applied, followed by a critical point drying treatment (Stokroos et al. 1998; Pathan et al. 2010). Finally, the samples were sputtered with a very thin layer of gold to improve the quality of the micrographs.

Statistical analysis

For this study, an ANOVA analysis was carried out using, at least, three replicates of each measure independently. In addition, a means comparison test was performed to detect significant differences ($p < 0.05$).

Results

Physicochemical properties of KL/CA solutions

As well-known, electrospinning performance depends on the physicochemical properties of the feeding solution (Salas 2017; Rubio-Valle et al. 2021a). Numerous researchers have reported the influence of surface tension, electrical conductivity, and viscosity of the solution on the morphological properties of electrospun nanofibers (Wang et al. 2013; Dallmeyer

et al. 2014). These properties, which are crucial and, in some cases, limiting factors for electrospinnability, mainly depend on the nature and concentration of the polymers used (Kakoria and Sinha-Ray 2018). Figure 1a shows the values of surface tension and electrical conductivity for the KL/CA solutions used in this study as feed for electrospinning. The surface tension ranges from 28.91 to 35.15 mN/cm, which is significantly higher than the surface tension of the DMF/Ac solvent mixture (23.64 mN/cm). Regarding the lignin origin, the surface tension of EKL/CA and PKL/CA solutions are not significantly different, however, OKL/CA solutions show higher surface tension values, probably due to the higher carbohydrate content (García-Fuentevilla et al. 2022). In addition, an increase in the CA proportion leads to an increase in surface tension. On the other hand, the electrical conductivity of the solutions ranges from 135.5 to 365.1 µS/cm, being again very similar for EKL/CA and PKL/CA solutions and, in this case, much higher for OKL/CA solutions. These high values of electrical conductivity must be associated with the higher residue percentage (basically inorganic salts) found in the OKL sample from TGA measurements (García-Fuentevilla et al. 2022). On the contrary, the higher the KL/CA ratio, the higher the electrical conductivity is, as a consequence of the lower molecular weight and more polar character of lignins comprising multiple phenolic and aliphatic hydroxyl and carboxyl groups (García-Fuentevilla et al. 2022).

All KL/CA solutions exhibit a Newtonian behavior in the range of shear rates applied (see Figure S1 in the supplementary material). As can be observed in Table 2, shear viscosity values increase with CA proportion, as a consequence of the higher CA molecular weight, which corroborates previously reported findings for other lignin/polymer blends (Aslanzadeh et al. 2016; Akbari et al. 2021; Borrego et al. 2021). Once again, it is observed that EKL/CA and PKL/CA solutions present similar viscosity values whereas OKL/CA solutions show significantly higher viscosity (0.181 and 0.475 Pa.s for 9:1 and 7:3 O KL:CA weight ratio, respectively). This can be attributed to the chemical composition and structural features of this particular Kraft lignin, which shows slightly lower polydispersity in the molecular weight distribution (M_w/M_n) and especially a higher amount of carbohydrates (García-Fuentevilla et al. 2022), mainly cellulose and hemicellulose (see also

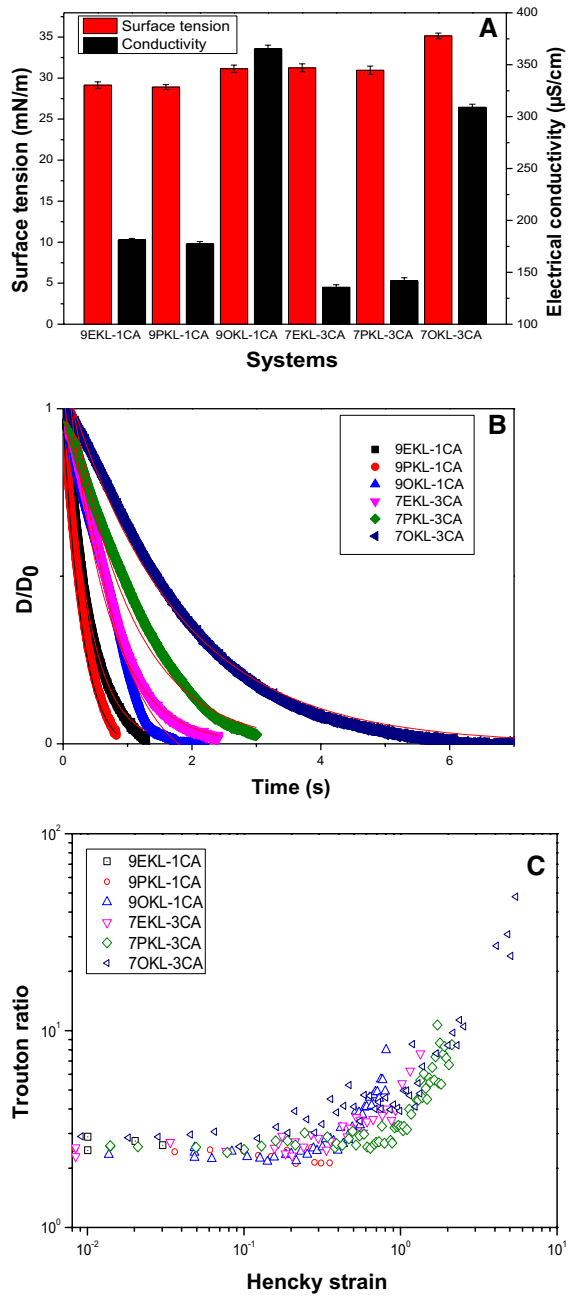

Fig. 1 **a** Surface tension and electrical conductivity, **b** evolution of normalized filament diameter with time and **c** Trouton ratio vs. Hencky strain plots in the transient extensional experiments for KL/CA solutions in DMF/Ac at 30 wt. %

total lignin content in Table 1). In addition, the OKL sample shows a significantly lower value of the syringyl/guaiacyl (S/G) ratio (Table 1), which has been reported to give rise to more cross-linkages, in turn

Table 2 Shear viscosity, extensional viscosity and relaxation time (λ) values of the different KL/CA solutions

KL:CA weight ratio	Kraft lignins	η (Pa.s)	$\eta_{ext,0}$ (Pa.s)	λ (s)
9:1	EKL	0.061^{α}	0.183^{a}	0.12^{A}
	PKL	0.055^{α}	0.165^{a}	0.09^{A}
	OKL	0.181^{β}	0.543^{b}	0.21^{B}
7:3	EKL	0.317^{γ}	0.951^{c}	0.36^{C}
	PKL	0.294^{γ}	0.882^{c}	0.24^{B}
	OKL	0.475^{δ}	1.425^{d}	0.52^{D}

Values differing in the superscripts are significantly different ($p < 0.05$)

yielding higher viscosity values in the melt state (Sun et al. 2016).

In addition, the extensional properties of the different KL/CA solutions were also evaluated by capillary breakthrough experiments. Figure 1b displays the evolution of the filament diameter, D(t), normalized with the initial filament diameter, D_0, as a function of KL/CA weight ratio and lignin origin. A quick filament thinning, almost linear at the beginning, characteristic of Newtonian liquids, was found for the lower KL:CA weight ratio studied, and especially for EKL/CA and PKL/CA solutions, while a more gradual exponential decay of filament diameter, typical of viscoelastic fluids, was observed for the higher KL:CA ratio. Dallmeyer et al. (2014) suggested that a useful parameter to account for the entire filament thinning process is the characteristic relaxation time, λ, which can be calculated by fitting filament thinning profiles to Eq. (1) (Fig. 1b).

$$\frac{D(t)}{D_0} = Ae^{-(t/3\lambda)} \tag{1}$$

where D(t) is the diameter measured as a function of time in the CaBER rheometer at the filament midpoint, D_o the initial filament diameter, σ the surface tension, and A a fitting parameter.

The characteristic relaxation times of the different KL/CA solutions studied are shown in Table 2. Several authors such as Borrego et al (2021) and Dallmayer et al. (2014) ascribed the success or failure in obtaining uniform fibers to the extensional properties of lignin/dopant solutions, suggesting a threshold value of the characteristic relaxation time, λ, of ~ 12 ms for the transition from predominant beaded structures to nanofibers. This relaxation time typically increases with total polymer concentration and dopant polymer: lignin ratio. As may be observed in Table 2, relaxation times of around 8–18 times this critical value was obtained for solutions prepared with a 9:1 KL:CA weight ratio, and much higher when using a 7:3 KL:CA ratio. In addition, since reasonably constant values of extensional viscosity were obtained on a short time scale, the limiting extensional viscosity values ($\eta_{ext,0}$) were also given in Table 2. The extensional viscosity is shown in the form of the Trouton ratio ($Tr = \eta_{ext}/\eta$) and plotted in Fig. 1c versus the Henckey strain. As may be appreciated, the theoretical value of $Tr = 3$ was reasonably met at low strains, i.e. the Hencky interval, and then the extensional viscosity progressively increases with the strain. This is mainly because capillary extensional processes are inherently transient phenomena, where the apparent extensional viscosity rises continually when changing from coiled to stretched states (Yu et al. 2006). In the case of EKL and PKL samples having 9:1 KL:CA ratio, i.e. small CA proportion, the Trouton ratio remained constant with low values (around 3) until filament breakage, accounting for the difficulty of lignin to undergo the transition from the coiled to a stretched state. However, the 9OKL-1CA sample does show an exponential increase in the Trouton ratio, similarly to that found in samples with 7:3 KL:CA ratio. As expected, both the characteristic relaxation time and limiting extensional viscosity increase with CA content, also reaching noticeably higher values for the solutions prepared with OKL.

Morphology of electrospun KL/CA nanostructures

Figure 2 presents the SEM micrographs of the electrospun nanostructures obtained from 30 wt.% polymer solutions as a function of the type of Kraft lignin and KL:CA weight ratio. As can be seen, beaded nanofibers (BOAS) networks with eventually embedded micrometer-sized particles were generated by adding a relatively small amount of CA (10 wt%) to lignin solutions (Figs. 2a, c and e). The amount and density of fibers increased considerably by increasing the CA concentration in KL:CA solutions (Figs. 2b, d and f), as a result of the enhanced rheological properties, i.e. higher shear and extensional viscosities and relaxation times (see Table 2). However, as can be observed, 7EKL-3CA and 7PKL-3CA nanostructures

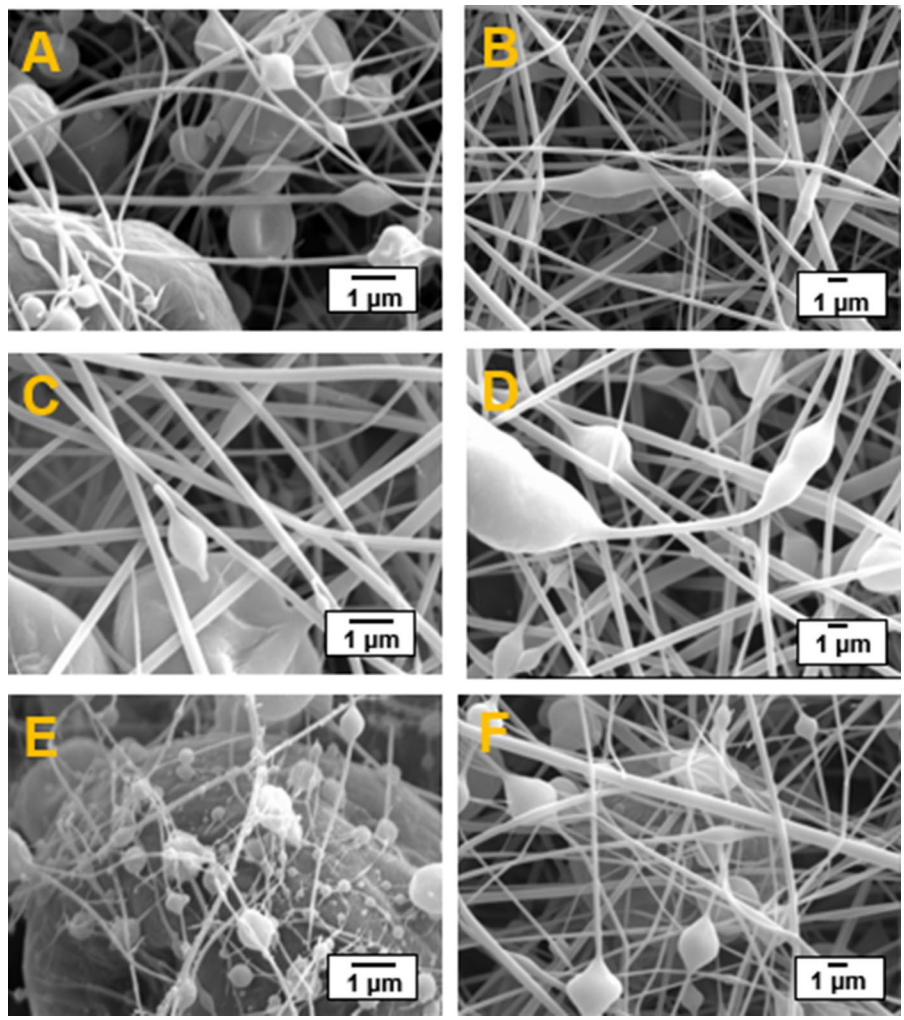

Fig. 2 SEM images of KL/CA electrospun nanostructures obtained from solutions with 30 wt.% total polymer concentration, differing in lignin source and KL:CA weight ratio. **a** 9EKL-1CA at × 10,000 magnification, **b** 7EKL-3CA at × 4000 magnification, **c** 9PKL-1CA at × 10,000 magnification, (D) 7PKL-3CA at × 4000 magnification, **e** 9OKL-1CA at × 10,000 magnification and **f** 7OKL-3CA at × 4000 magnification

reveal some nanometer-sized and elongated beads as part of the filaments, but not large and isolated particles, which are instead visible in the 7OKL-3CA morphology.

Table 3 shows the average particle and fiber diameters, obtained from the size distributions deduced from SEM images, as well as the overall porosity of the nanostructures. As can be seen, an increase in the average fiber diameter was always observed by increasing the CA content, which is also associated with a significant decrease in the average particle (or bead) diameter. In addition, thinner filaments and larger particles were found with the OKL lignin, whereas thicker fibers and more uniform nanostructures were generally observed in EKL/CA and PKL/CA systems. On the other hand, due to the lower amount of particles and/or beads in the filaments, the

Table 3 Average particle and fiber diameters and overall porosity of electrospun EKL/CA, PKL/CA and OKL/CA nanostructures at different KL: CA weight ratio

SYSTEMS	Average diameters of particle or beads (µm)	Average fibers diameters (µm)	Porosity (%)
9EKL-1CA	2.1^{a}	0.29^{A}	36.1^{α}
9PKL-1CA	2.3^{a}	0.27^{A}	31.6^{δ}
9OKL-1CA	4.5^{b}	0.12^{B}	23.5^{β}
7EKL-3CA	0.36^{c}	0.61^{C}	46.63^{γ}
7PKL-3CA	0.41^{c}	0.54^{C}	45.78^{γ}
7OKL-3CA	0.97^{d}	0.33^{D}	37.19^{α}

Values differing in the superscripts are significantly different ($p < 0.05$)

nanostructure porosity increases with CA content, being higher when using EKL or PKL lignins. These results are in agreement with the physicochemical properties and relaxation times of the spinning solutions, which are similar for EKL/CA and PKL/CA solutions thus yielding similar morphological properties of the resulting electrospun nanostructures. On the contrary, OKL/CA electrospun morphologies are rather different, exhibiting a higher amount of particles and/or beaded fibers, despite the higher shear and extensional viscosity values found in the solutions. Possibly, these discrepancies are due to the very high values in the electrical conductivity that these solutions showed, which cause the formation of unstable Taylor cones (Angammana and Jayaram 2011; Li and Wang 2013).

In order to understand the influence of the chemical structure and composition of the Kraft lignins on the morphological properties of electrospun nanostructures, the data shown in Table 1 must be taken into account. Thus, OKL sample significantly differs from EKL and PKL samples, which have more comparable structural and compositional characteristics. For instance, EKL and PKL show a higher content of β-O-4' substructures, which implies more linear (less branched) chemical structures that may help to improve the spinnability. Moreover, the abundance of S units, compared to G units in EKL and PKL, has been reported to be beneficial to enhance the spinnability of lignins (Du et al. 2021). Finally, the worse performance of the OKL sample during the electrospinning process must be mainly attributed to the extremely high electric conductivity provided by the salt content.

Castor oil structuring properties of electrospun EKL/CA nanostructures

Recent studies have demonstrated that electrosprayed lignin nanoparticles, i.e. non-fibrous structures composed only of micro- or nanometer-sized particles, give rise to weak and unstable physical interactions in a vegetable oil medium, inexorably resulting in phase separation (Borrego et al. 2021; Rubio-Valle et al. 2021b), whereas electrospun nanofiber mats were able to generate physically stable oleogels. This is mainly due to the fact that oil structuring basically occurs through the formation of a percolation network with enhanced physical interactions as a consequence of the large specific surface area and the high aspect ratio of nanofibers. These interactions involved in oil structuring are mainly intermolecular hydrophobic and Van der Waals forces (Ding et al. 2006). As a result, by simple gentle mechanical dispersion of the electrospun nanostructures in castor oil, the oil becomes entrapped in the generated voids and swells to some extent. The microstructures of resulting oleogels prepared with 15 wt. % KL/CA electrospun nanostructures are shown in Fig. 3. As can be seen, uniform networks composed predominantly of fibers or BOAS are apparent in all the samples. Figures 3a, c and e show micrographs of oleogels prepared with electrospun 9KL/1CA nanostructures employing EKL, PKL and OKL lignins, respectively. According to the electrospun nanostructures shown in Fig. 2, these morphologies comprise more heterogeneous BOAS networks, with eventually micrometer-sized particles, especially in the case of oleogel sample prepared with 9OKL-1CA. On the contrary, predominant homogenous fiber networks can be visualized in the microstructures of oleogels prepared with 7EKL-3CA, 7PKL-3CA and 7OKL-3CA samples (Figs. 3b, d and f, respectively). Apparently, the gentle mechanical agitation applied to disperse the nanofibers into the oil does not affect fiber length. The main effect observed upon dispersing the nanofibers was the swelling of these.

Table 4 shows the average fiber diameters obtained from the analysis of oleogel SEM images, as well as the degree of swelling defined as:

$$\beta = \frac{D_{f\_}D_0}{D_f} \tag{2}$$

where D_o refers to the average diameter of electrospun nanostructures and D_f to average diameters of KL/CA fibers in the oil medium. According to this, fiber diameter considerably increases in the percolation network as a consequence of oil-induced swelling, being more significant in those oleogels prepared using an electrospun 9KL/1CA nanostructures and particularly the OKL lignin. Overall, the microstructure of oleogels is mainly governed by the morphological properties of electrospun nanostructures used as structuring agents.

The rheological properties of these oleogels are largely determined by the electrospun nanostructures and structural features of Kraft lignins.

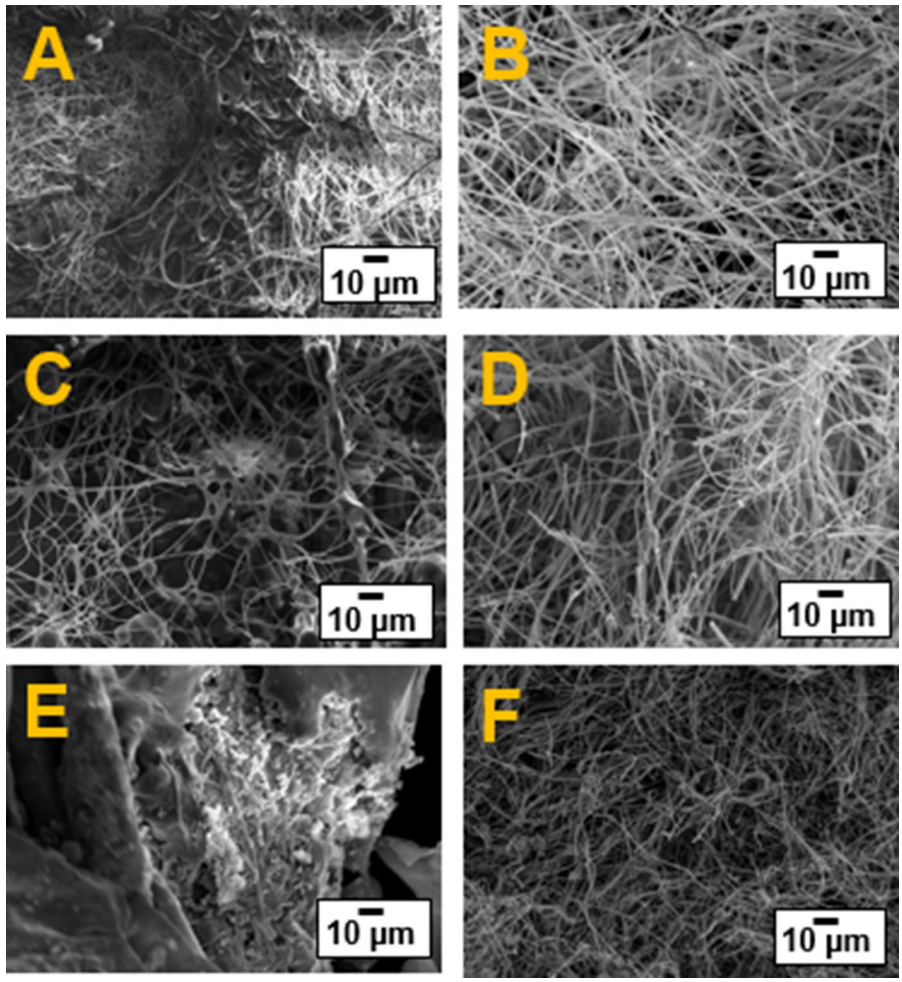

Fig. 3 SEM images of oleogels obtained with electrospun KL/CA nanostructures as a function of the lignin type and CA content. **a** O-9EKL-1CA, **b** O-7EKL-3CA, **c** O-9PKL-1CA, **d** O-7PKL-3CA, **e** O-9OKL-1CA and **f** O-7OKL-3CA at × 1000 magnification

Table 4 Average fiber diameter and degree of swelling (β) of oleogels fibers

Oleogels	Average fiber diameter (µm)	Swelling factor β (%)
O-9EKL-1CA	1.31^{a}	77.86^{A}
O-9PKL-1CA	1.25^{a}	78.40^{A}
O-9OKL-1CA	0.98^{b}	93.94^{B}
O-7EKL-3CA	1.47^{c}	58.50^{C}
O-7PKL-3CA	1.41^{c}	61.70^{C}
O-7OKL-3CA	1.05^{d}	68.57^{D}

Values differing in the superscripts are significantly different ($p < 0.05$)

Figures 4a and b show the mechanical spectra of the oleogels obtained from the dispersion of electrospun KL/CA nanostructures, at 15 wt%, in castor oil, as a function of lignin source and CA content. The evolution of the SAOS functions, i.e. the storage modulus, G', and the loss modulus, G", with frequency is characteristic of gel-like dispersions and qualitatively similar for all the samples studied, with G' always higher than G" over the entire frequency range studied. Although the values of the SAOS functions in traditional lubricating greases basically depend on the type and concentration of the thickener, the mechanical spectra achieved for these oleogels are very similar to those displayed for the most commonly employed NLGI 1–2 grade lubricating greases, typically showing G' values of 10^4–10^5 Pa, and G" around one order of magnitude lower (Delgado et al. 2006). On the one hand, by comparing the oleogels containing nanostructures with different KL:CA weight ratios, it is clearly observed that increasing the CA proportion leads to

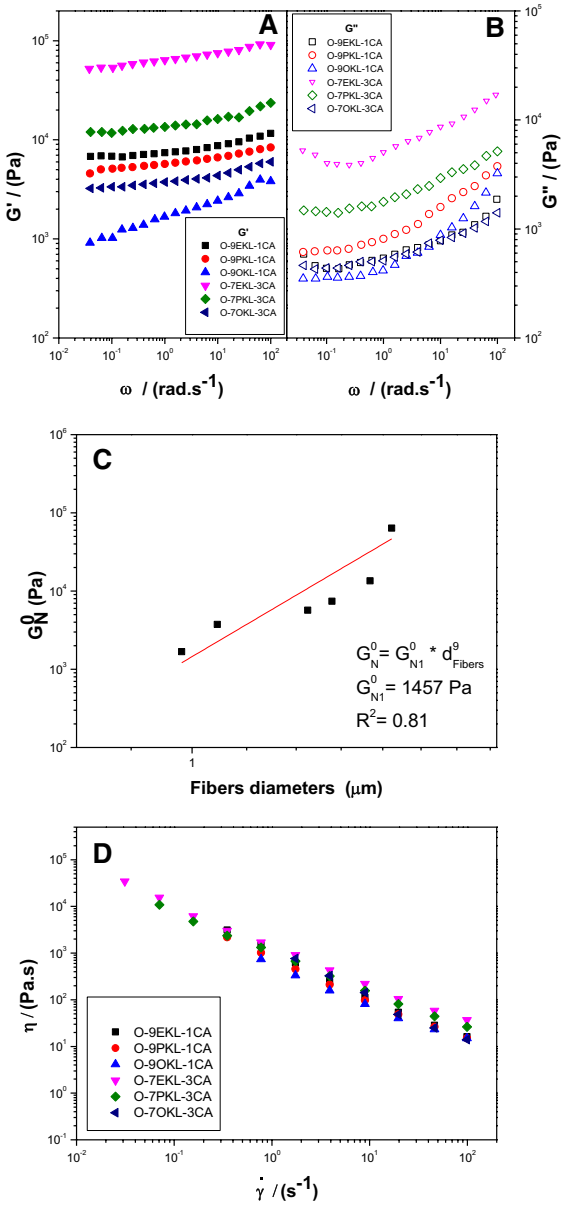

Fig. 4 Evolution of **a** the storage modulus, G' and **b** the loss modulus, G" with frequency for oleogels as a function of KL:CA weight ratio and lignin source, **c** influence of average fiber diameter on the plateau modulus of oleogels, and **d** viscous flow curves for oleogels as a function of KL:CA weight ratio and lignin source

an enhancement of the gel strength, i.e. an increase in the values of the SAOS functions and higher relative elasticity (lower values of the loss tangent). These results may be explained by attending to two factors, the higher proportion of the component with the higher average molecular weight (CA) and the increase of porosity and fiber diameter in electrospun nanostructures. Regarding the lignin source, the higher viscoelastic functions were obtained with EKL/CA nanostructures, followed by PKL/CA and finally OKL/CA, which is essentially a consequence of the morphological characteristics discussed above. In this sense, Fig. 4c illustrates the dependence of the plateau modulus (G_N^0) on the average fiber diameter in the percolation network. As can be seen, G_N^0 potentially increases with fiber diameter. This dependence may be fitted quite well to a power-law equation, with adjustable parameters ($G^o_{N,1}$ and b) shown in the inset of Fig. 5c:

$$G_N^o = G_{N,1}^o D_f^b \tag{3}$$

Therefore, the morphological characteristics of the electrospun nanostructures determine the rheological properties of resulting oleogels, which can be modulated with the composition of the lignin used as structuring agent and electrospinning conditions.

Regarding the viscous flow response, a shear-thinning behavior was always displayed in the shear rate range studied, which may be fairly well depicted by the power-law model:

$$\eta = K\dot{\gamma}^{n-1} \tag{4}$$

where K y n are the consistency and flow indexes, respectively. Figure 4d shows the viscous flow curves for oleogels prepared with KL/CA electrospun nanostructures. The corresponding K and n values are listed in Table 5. As can be noticed, very similar viscous flow responses were obtained regardless lignin source and KL:CA weight ratio. As expected, higher K values were obtained by increasing the CA content. Moreover, once again, oleogels prepared with OKL/CA nanostructures provide lower values of consistency index in comparison with EKL/CA and PKL/CA-based nanostructures. On the other hand, very low values of the flow index, n, were generally obtained, pointing out that oleogels exhibit a markedly shear thinning behaviour, which also resembles the yielding behaviour exhibited by traditional lubricating greases (Delgado et al. 2006).

Table 5 Values of consistency and flow indexes, friction coefficient and wear scar diameter for oleogels prepared with electrospun KL/CA nanostructures of different Kraft lignins and KL:CA weight ratio. The friction coefficient and wear scar diameter values for pure castor oil were also included for the sake of comparison

Oleogels	K (Pa.s^n)	n	Friction coefficient	Wear scar diameter (μm)
O-9EKL-1CA	971.5^{AA}	0.11^{Aa}	0.092^{a}	281.16^{A}
O-9PKL-1CA	793.2^{BB}	0.09^{Bb}	0.076^{b}	193.31^{B}
O-9OKL-1CA	576.1^{CC}	$0,06^{Cc}$	0.070^{b}	148.76^{C}
O-7EKL-3CA	1347.1^{DD}	0.24^{Dd}	0.124^{c}	385.75^{D}
O-7PKL-3CA	1123.1^{EE}	0.23^{Dd}	0.116^{c}	317.92^{E}
O-7OKL-3CA	715.2^{BB}	0.08^{Aa}	0.107^{c}	297.97^{A}
Castor oil*			0.083	508.7

Values differing in the superscripts are significantly different ($p < 0.05$)

* From Delgado et al. (2020)

Tribological performance of electrospun EKL/CA nanostructures-based oleogels

Finally, the lubrication performance of these oleogels was assessed in a steel-steel ball-on-plates tribological contact by analyzing friction and wear. The values of the friction coefficient over time were recorded at constant axial load and a rotational speed (20 N and 10 rpm) and the average values are shown in Table 5 for the different electrospun nanostructures, together with the average wear scar size generated on plates. Most of the oleogel samples yield acceptable friction coefficient values and wear diameters, which are quite similar to those reported for commercial lubricating greases (Zhang et al. 2018; Sánchez et al. 2014) and oleogels obtained with chemically functionalized biopolymers (Borrero-López et al. 2020; Cortés-Triviño et al. 2019) under similar conditions. In order to assess the influence of the structuring agent, i.e. the electrospun nanostructures, the values of the friction coefficient and average wear scar diameter for pure castor oil were also included in Table 5. The higher proportion of CA in nanofibers, the higher friction coefficient and wear size was obtained. Moreover, oleogels prepared with OKL lignin-based nanostructures provide particularly low values of friction coefficient and wear scar diameters in comparison with EKL and PKL lignins. As in the case of the rheological properties, the tribological response is essentially governed by the morphological characteristics of the electrospun nanostructures, i.e. fiber diameter, number of beads and porosity. In this regard, OKL/CA nanostructures comprising lower fiber diameters and a higher number of beads and/or isolated particles are possibly mechanically weaker, which allows the oil to be released more easily in the lubricated contact. In general, the higher fiber diameter, the higher the friction coefficient and wear scar size. Moreover, it is worth mentioning that although 9EKL-1CA has a similar fiber diameter to 9PKL-1CA, it presents significantly higher friction coefficients, probably due to a greater capacity to hold the oil in its voids as it has a higher overall porosity. Finally, as can be seen, the friction coefficient provided by pure castor oil is similar to that obtained with nanostructures having 9:1 KL:CA ratio, which supports the hypothesis that the better tribological performance is related to the ability of the nanostructure to release the oil easily. However, as expected, oil structuring with KL/CA nanostructures results in much better preservation of metallic surfaces against wear compared to pure castor oil.

Concluding remarks

Solutions of Kraft lignins (KL) from different sources such as eucalyptus (EKL), poplar (PKL) and olive tree pruning (OKL), and cellulose acetate (CA) in a 1:2 v/v mixture of DMF and acetone, using 9KL:1CA and 7KL:3CA weight ratios, were prepared and used as feed for electrospinning. The morphology of the resulting electrospun KL/CA nanostructures is highly dependent on the physico-chemical properties of the spinning solutions, the KL:CA weight ratio and the chemical and compositional characteristics of the Kraft lignins. In general, EKL/CA and PKL/CA solutions have similar physico-chemical properties, according to their comparable chemical structures and composition, which give rise to similar electrospun nanostructures. On the contrary, OKL/CA solutions has higher shear and extensional viscosity, mainly due to a higher carbohydrate content, but lower electrospinning performance, which was mainly attributed to an excessively high electrical conductivity as a consequence of high salt content. Surface tension, shear viscosity and extensional properties of KL/CA solutions

increase with the CA proportion, whereas electrical conductivity increases with the lignin content.

Beaded nanofiber (BOAS) networks with eventually embedded micrometer-sized particles were produced when using a 9:1 KL:CA ratio, whilst more homogeneous nanofiber mats were obtained with a 7:3 KL:CA weight ratio. Thicker fibers and more uniform nanostructures were generally produced from EKL/CA and PKL/CA solutions, which generally yielded better electrospinning performance. In addition, the porosity of nanofiber networks increases with CA content, being also higher when using EKL or PKL lignins instead of OKL.

The electrospun KL/CA mats consisting of filament-interconnected particles and especially more uniform nanofibers networks are able to successfully structure castor oil, resulting in gel-like dispersions. The swelling of KL/CA nanofibers in the percolation network was demonstrated. The rheological and tribological properties of these oleogels essentially depend on the morphological characteristics of the electrospun KL/CA nanostructures rather than the chemistry of individual fibers. A correlation between the plateau modulus of oleogels and fiber diameters was derived.

Overall, the oleogels based on KL/CA nanostructures showed appropriate rheological and tribological properties, comparable to those of conventional lubricating greases. However, the oleogel prepared with an electrospun nanostructure consisting of a relatively weak BOAS morphology exhibited exceptionally low friction coefficient values and reduced wear scar diameters, as a probable result of the oil being released more efficiently in the lubricating contact zone, dictated by the lower porosity and reduced diameter exhibited by these kinds of nanostructures.

Acknowledgments This work is part of a research project (RTI2018-096080-B-C21) funded by MCIN/AEI/10.13039/501100011033 and by "ERDF A way of making Europe". J.F. Rubio-Valle has also received a Ph.D. Research Grant PRE2019-090632 from Ministerio de Ciencia e Innovación (Spain). The financial support is gratefully acknowledged.

Author contributions All authors contributed to the study conception and design. J.F.R.V. did experimental work, wrote original manuscript and prepared Figures and Tables. C.V. did experimental work, wrote original and reviewed manuscript and Figures. M.C.S. reviewed manuscript and Figures. J.E.M.A. did experimental work and reviewed manuscript and Figures. J.M.F. wrote original manuscript, reviewed final version and supervised experimental work. All authors read and approved the final manuscript.

Funding Open Access funding provided by Universidad de Huelva/CBUA thanks to the CRUE-CSIC agreement with Springer Nature. This work was funded by MCIN/AEI/10.13039/501100011033 and by "ERDF A way of making Europe" (Project RTI2018-096080-B-C21). J.F. Rubio-Valle. has also received a Ph.D. Research Grant PRE2019-090632 from Ministerio de Ciencia e Innovación (Spain).

Data availability All of the material is owned by the authors and no permissions are required. All the data and materials will be made available if required.

Declarations

Conflict of interest The authors have no relevant financial or non-financial interests to disclose.

Ethics approval and consent to participate Not applicable.

Consent for publication Consent of publication has been taken from all authors. Authors read and understood the publishing policy, and submit this manuscript in accordance with this.

References

Akbari S, Bahi A, Farahani A et al (2021) Fabrication and characterization of lignin/dendrimer electrospun blended fiber mats. Molecules 26:518. https://doi.org/10.3390/molecules26030518

Angammana CJ, Jayaram SH (2011) Analysis of the effects of solution conductivity on electrospinning process and fiber morphology. IEEE Trans Ind Appl 47:1109–1117. https://doi.org/10.1109/TIA.2011.2127431

Aslanzadeh S, Zhu Z, Luo Q et al (2016) Electrospinning of colloidal lignin in poly(ethylene oxide) N, N -*Dimethylformamide* solutions. Macromol Mater Eng 301:401–413. https://doi.org/10.1002/mame.201500317

Bajpai P (2016) Structure of Lignocellulosic Biomass. Pp. 7–12

Borrego M, Martín-Alfonso JE, Sánchez MC et al (2021) Electrospun lignin-PVP nanofibers and their ability for

structuring oil. Int J Biol Macromol 180:212–221. https://doi.org/10.1016/j.ijbiomac.2021.03.069

Borrero-López AM, Blánquez A, Valencia C et al (2018a) Valorization of soda lignin from wheat straw solid-state fermentation: production of *Oleogels*. ACS Sustain Chem Eng 6:5198–5205. https://doi.org/10.1021/acssuschemeng.7b04846

Borrero-López AM, Santiago-Medina FJ, Valencia C et al (2018b) Valorization of Kraft lignin as thickener in castor oil for lubricant applications. J Renew Mater 6:347–361. https://doi.org/10.7569/JRM.2017.634160

Borrero-López AM, Valencia C, Blánquez A et al (2020) Cellulose pulp- and castor oil-based polyurethanes for lubricating applications: influence of streptomyces action on barley and wheat straws. Polym Basel 12:2822. https://doi.org/10.3390/polym12122822

Borrero-López AM, Valencia C, Franco JM (2022) Lignocellulosic materials for the production of biofuels, biochemicals and biomaterials and applications of lignocellulose-based polyurethanes: a review. Polym Basel 14:881. https://doi.org/10.3390/polym14050881

Boyde S (2002) Green lubricants. environmental benefits and impacts of lubrication. Green Chem 4:293–307. https://doi.org/10.1039/b202272a

Cai J, He Y, Yu X et al (2017) Review of physicochemical properties and analytical characterization of lignocellulosic biomass. Renew Sustain Energy Rev 76:309–322. https://doi.org/10.1016/j.rser.2017.03.072

Cara C, Ruiz E, Oliva JM et al (2008) Conversion of olive tree biomass into fermentable sugars by dilute acid pretreatment and enzymatic saccharification. Bioresour Technol 99:1869–1876. https://doi.org/10.1016/j.biortech.2007.03.037

Cortés-Triviño E, Valencia C, Delgado MA, Franco JM (2019) Thermo-rheological and tribological properties of novel bio-lubricating greases thickened with epoxidized lignocellulosic materials. J Ind Eng Chem 80:626–632. https://doi.org/10.1016/j.jiec.2019.08.052

Cortés-Triviño E, Valencia C, Franco JM (2021) Thickening castor oil with a lignin-enriched fraction from sugarcane bagasse waste via epoxidation: a rheological and hydrodynamic approach. ACS Sustain Chem Eng 9:10503–10512. https://doi.org/10.1021/acssuschemeng.1c02166

Dallmeyer I, Ko F, Kadla JF (2014) Correlation of elongational fluid properties to fiber diameter in electrospinning of softwood Kraft lignin solutions. Ind Eng Chem Res 53:2697–2705. https://doi.org/10.1021/ie403724y

Davidovich-Pinhas M, Barbut S, Marangoni AG (2015) The gelation of oil using ethyl cellulose. Carbohydr Polym 117:869–878. https://doi.org/10.1016/j.carbpol.2014.10.035

Delgado MA, Valencia C, Sánchez MC et al (2006) Influence of soap concentration and oil viscosity on the rheology and microstructure of lubricating greases. Ind Eng Chem Res 45:1902–1910. https://doi.org/10.1021/ie050826f

Delgado MA, Cortés-Triviño E, Valencia C, Franco JM (2020) Tribological study of epoxide-functionalized alkali lignin-based gel-like biogreases. Tribol Int 146:106231. https://doi.org/10.1016/j.triboint.2020.106231

Diez-Rodríguez G, Hübner L, Antunes L, Nava D (2013) *Herpetogramma bipunctalis* (*Lepidoptera*: *Crambidae*) biology and techniques for rearing on leaves of the blackberry (*Rubus* spp., *Rosaceae*). Braz J Biol 73:179–184. https://doi.org/10.1590/S1519-69842013000100019

Ding B, Li C, Hotta Y et al (2006) Conversion of an *Electrospun nanofibrous* cellulose acetate mat from a super-hydrophilic to super-hydrophobic surface. Nanotechnology 17:4332–4339. https://doi.org/10.1088/0957-4484/17/17/009

Du B, Zhu H, Chai L et al (2021) Effect of lignin structure in different biomass resources on the performance of lignin-based carbon nanofibers as supercapacitor electrode. Ind Crops Prod 170:113745. https://doi.org/10.1016/j.indcrop.2021.113745

Gallego R, Arteaga JF, Valencia C, Franco JM (2013) Chemical modification of methyl cellulose with HMDI to modulate the thickening properties in castor oil. Cellulose 20:495–507. https://doi.org/10.1007/s10570-012-9803-4

García-Fuentevilla L, Rubio-Valle JF, Martín-Sampedro R et al (2022) Different Kraft lignin sources for *Electrospun* nanostructures production: influence of chemical structure and composition. Int J Biol Macromol 214:554–567. https://doi.org/10.1016/j.ijbiomac.2022.06.121

Gellerstedt G, Henriksson G (2008) Lignins: Major Sources, Structure and Properties. In: Monomers, Polymers and Composites from Renewable Resources. Elsevier, pp. 201–224

Gnansounou E (2010) Production and use of lignocellulosic bioethanol in Europe: current situation and perspectives. Bioresour Technol 101:4842–4850. https://doi.org/10.1016/j.biortech.2010.02.002

Heyer P, Läuger J (2009) Correlation between friction and flow of lubricating greases in a new tribometer device. Lubr Sci 21:253–268. https://doi.org/10.1002/ls.88

Jedrzejczyk MA, Van den Bosch S, Van Aelst J et al (2021) Lignin-based additives for improved thermo-oxidative stability of *Biolubricants*. ACS Sustain Chem Eng 9:12548–12559. https://doi.org/10.1021/acssuschemeng.1c02799

Jia H, Sun N, Dirican M et al (2018) Electrospun Kraft lignin/cellulose acetate-derived nanocarbon network as an anode for high-performance sodium-ion batteries. ACS Appl Mater Interfaces 10:44368–44375. https://doi.org/10.1021/acsami.8b13033

Kakoria A, Sinha-Ray S (2018) A Review on biopolymer-based fibers via electrospinning and solution blowing and their applications. Fibers 6:45. https://doi.org/10.3390/fib6030045

Kobayashi H, Fukuoka A (2013) Synthesis and utilisation of sugar compounds derived from lignocellulosic biomass. Green Chem 15:1740. https://doi.org/10.1039/c3gc00060e

Lainez M, González JM, Aguilar A, Vela C (2018) Spanish strategy on bioeconomy: towards a knowledge based sustainable innovation. N Biotechnol 40:87–95. https://doi.org/10.1016/j.nbt.2017.05.006

Laurichesse S, Avérous L (2014) Chemical modification of lignins: towards biobased polymers. Prog Polym Sci 39:1266–1290. https://doi.org/10.1016/j.progpolymsci.2013.11.004

Lewandowski I (ed) (2018) Bioeconomy. Springer International Publishing, Cham

Li Z, Wang C (2013) Effects of Working Parameters on Electrospinning. pp. 15–28

Limayem A, Ricke SC (2012) Lignocellulosic biomass for bioethanol production: Current perspectives, potential issues and future prospects. Prog Energy Combust Sci 38:449–467. https://doi.org/10.1016/j.pecs.2012.03.002

Liu H, Hsieh Y-L (2002) Ultrafine fibrous cellulose membranes from electrospinning of cellulose acetate. J Polym Sci Part B Polym Phys 40:2119–2129. https://doi.org/10.1002/polb.10261

Martín-Alfonso JE, Núñez N, Valencia C et al (2011) Formulation of new biodegradable lubricating greases using ethylated cellulose pulp as thickener agent. J Ind Eng Chem 17:818–823. https://doi.org/10.1016/j.jiec.2011.09.003

Negro MJ, Manzanares P, Ruiz E, et al (2017) The biorefinery concept for the industrial valorization of residues from olive oil industry. In: Olive Mill Waste. Elsevier, pp. 57–78

Obst JR (1983) Analytical pyrolysis of hardwood and softwood lignins and its use in lignin-type determination of hardwood vessel elements. J Wood Chem Technol 3:377–397. https://doi.org/10.1080/02773818308085170

Octave S, Thomas D (2009) *Biorefinery*: toward an industrial metabolism. Biochimie 91:659–664. https://doi.org/10.1016/j.biochi.2009.03.015

Pathan AK, Bond J, Gaskin RE (2010) Sample preparation for SEM of plant surfaces. Mater Today 12:32–43. https://doi.org/10.1016/S1369-7021(10)70143-7

Pelaez-Samaniego MR, Yadama V, Garcia-Perez M et al (2016) Interrelationship between lignin-rich dichloromethane extracts of hot water-treated wood fibers and high-density polyethylene (HDPE) in wood plastic composite (WPC) production. Holzforschung 70:31–38. https://doi.org/10.1515/hf-2014-0309

Quinchia LA, Delgado MA, Valencia C et al (2010) Viscosity modification of different vegetable oils with EVA copolymer for lubricant applications. Ind Crops Prod 32:607–612. https://doi.org/10.1016/j.indcrop.2010.07.011

Romero-García JM, Niño L, Martínez-Patiño C et al (2014) Biorefinery based on olive biomass. State of the art and future trends. Bioresour Technol 159:421–432. https://doi.org/10.1016/j.biortech.2014.03.062

Rubio-Valle JF, Sánchez MC, Valencia C et al (2021b) *Electrohydrodynamic* processing of PVP-doped Kraft lignin micro- and nano-structures and application of *Electrospun* nanofiber templates to produce *Oleogels*. Polymers (basel) 13:2206. https://doi.org/10.3390/polym13132206

Rubio-Valle JF, Jiménez-Rosado M, Perez-Puyana V, et al (2021a) Electrospun nanofibres with antimicrobial activities. In: Antimicrobial Textiles from Natural Resources. Elsevier, pp. 589–618

Salas C (2017) Solution electrospinning of nanofibers. In: Electrospun Nanofibers. Elsevier, pp 73–108

Sánchez R, Valencia C, Franco JM (2014) Rheological and tribological characterization of a new acylated chitosan-based biodegradable lubricating grease: a comparative study with traditional lithium and calcium greases. Tribol Trans 57:445–454. https://doi.org/10.1080/10402004.2014.880541

Shahzadi T, Mehmood S, Irshad M et al (2014) Advances in lignocellulosic biotechnology: a brief review on lignocellulosic biomass and cellulases. Adv Biosci Biotechnol 05:246–251. https://doi.org/10.4236/abb.2014.53031

Sørensen A, Lübeck M, Lübeck P, Ahring B (2013) Fungal beta-glucosidases: a bottleneck in industrial use of lignocellulosic materials. Biomolecules 3:612–631. https://doi.org/10.3390/biom3030612

Staffas L, Gustavsson M, McCormick K (2013) Strategies and policies for the bioeconomy and bio-based economy: an analysis of official national approaches. Sustainability 5:2751–2769. https://doi.org/10.3390/su5062751

Stokroos K, Der Want V, Jongebloed, (1998) A comparative study of thin coatings of Au/Pd, Pt and Cr produced by magnetron sputtering for FE-SEM. J Microsc 189:79–89. https://doi.org/10.1046/j.1365-2818.1998.00282.x

Sun S, Huang Y, Sun R, Tu M (2016) The strong association of condensed phenolic moieties in isolated lignins with their inhibition of enzymatic hydrolysis. Green Chem 18:4276–4286. https://doi.org/10.1039/C6GC00685J

Svinterikos E, Zuburtikudis I, Al-Marzouqi M (2020) Fabricating carbon nanofibers from a lignin/r-PET blend: the synergy of mass ratio with the average fiber diameter. Appl Nanosci 10:1331–1343. https://doi.org/10.1007/s13204-019-01235-7

Syahir AZ, Zulkifli NWM, Masjuki HH et al (2017) A review on bio-based lubricants and their applications. J Clean Prod 168:997–1016. https://doi.org/10.1016/j.jclepro.2017.09.106

Teixeira MA, Paiva MC, Amorim MTP, Felgueiras HP (2020) Electrospun nanocomposites containing cellulose and its derivatives modified with specialized biomolecules for an enhanced wound healing. Nanomaterials. https://doi.org/10.3390/nano10030557

Ullah K, Kumar Sharma V, Dhingra S et al (2015) Assessing the lignocellulosic biomass resources potential in developing countries: a critical review. Renew Sustain Energy Rev 51:682–698. https://doi.org/10.1016/j.rser.2015.06.044

Wang X, He G, Liu H, et al (2013) Fabrication and morphological control of electrospun ethyl cellulose nanofibers. 8th Annu IEEE Int Conf Nano/Micro Eng Mol Syst IEEE NEMS 2013 1:324–327. https://doi.org/10.1109/NEMS.2013.6559742

Xi Y, Yang D, Qiu X et al (2018) Renewable lignin-based carbon with a remarkable electrochemical performance from potassium compound activation. Ind Crops Prod 124:747–754. https://doi.org/10.1016/j.indcrop.2018.08.018

Yu JH, Fridrikh SV, Rutledge GC (2006) The role of elasticity in the formation of electrospun fibers. Polymer (guildf) 47:4789–4797. https://doi.org/10.1016/j.polymer.2006.04.050

Zhang J, Li J, Wang A et al (2018) Improvement of the tribological properties of a lithium-based grease by addition of graphene. J Nanosci Nanotechnol 18:7163–7169. https://doi.org/10.1166/jnn.2018.15511